FALL 1999

Volume 1 Number 2

Solutions

Software Applications for Engineering Simulation and Processes

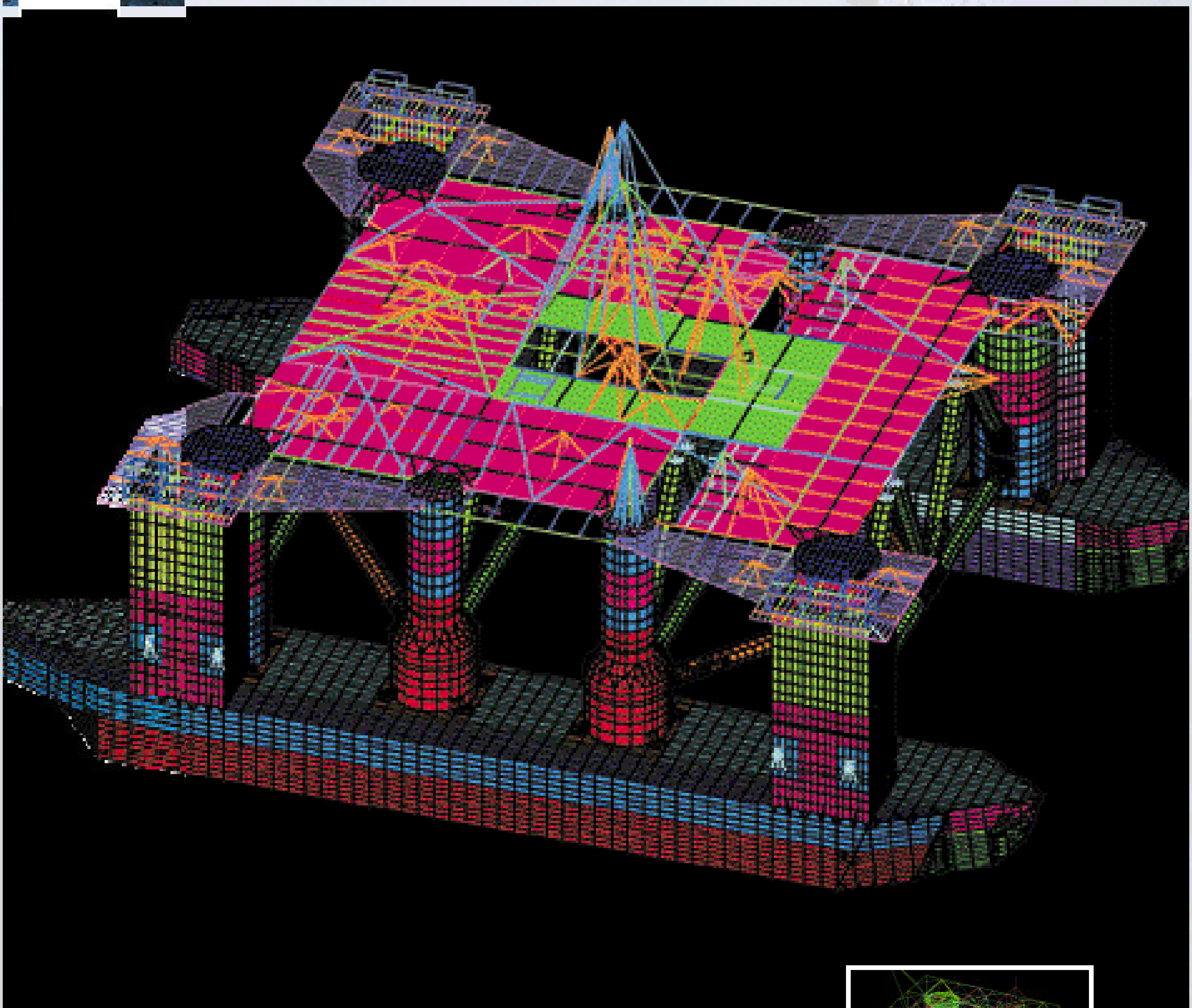

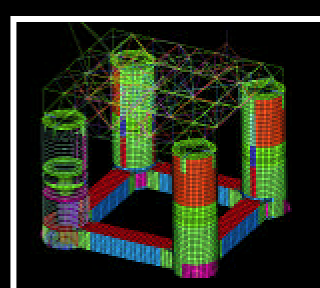

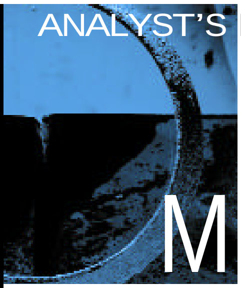

Modeling MEMS Resonant Devices Over a Broad Temperature Range

How temperature affects silicon carbide lateral resonators

By Russell DeAnna
U.S. Army Research Laboratory, NASA Glenn Research Center

Shuvo Roy,
Christian A. Zorman, and
Mehran Mehregany
Microfabrication Laboratory, Case Western Reserve University

MicroElectroMechanical Systems (MEMS) is a rapidly growing technology with a broad range of commercial applications and a diverse collection of evolving MEMS sensors and actuators. Lateral resonators comprise one class of MEMS devices that can be configured as electromechanical filters, gyroscopes, or accelerometers. Typical industrial applications are in the automotive industry for equipment such as air bag deployment, active suspension, and positioning/guidance systems. Lateral resonators are also among the standard devices used to determine mechanical properties like Young's modulus, residual stress, and structural damping coefficients. Micromachined polysilicon is the most commonly used material, however silicon carbide (SiC) potentially is a more attractive material for these devices because of its higher elastic modulus and excellent high-temperature mechanical and electrical properties.

The resonant frequency change with temperature has been used to calculate the temperature coefficient of Young's modulus. One experiment determined the resonant-frequency temperature coefficient for a polysilicon resonator of -17 ppm/°C. Other experiments found -25 ppm/°C for a polysilicon device on a Si substrate and -10 ppm/°C for a SiC device on a Si substrate.

According to theory, two temperature coefficients influence the resonant frequency of the typical, folded-beam resonator — Young's modulus and thermal expansion. When the device and substrate are made of different materials and the anchors are not located at a single point, the differential expansion between device and substrate creates thermal stress, and the resonant frequency deviates from theory. To gain an understanding of the importance of this thermal stress, two designs are considered: one with anchor locations close together and one where the anchor locations are far apart.

Temperature and Resonance

The resonant frequency of a folded-beam resonator is governed by

$$f_r^2 = 24EI/(L^3M) \qquad \text{(Eq. 1)}$$

where E is Young's modulus, I is the beam moment of inertia, L is the beam length, and M is the effective mass of the structure. M is constant with temperature and can be neglected in this discussion. Using the linear coefficient of thermal expansion α, and the Young's modulus temperature coefficient α_E, and the resonant frequency temperature coefficient α_{fr}, Equation 1 can be written as

$$(1+\alpha_{fr}T)^2 \propto (1\alpha_E T)(1+\alpha T) \qquad \text{(Eq. 2)}$$

where T is the temperature change. Expanding terms gives Equation 3.

$$(1+2\alpha_{fr}T+\alpha^2_{fr}T^2) \propto (1+(\alpha_E+\alpha)T+\alpha_E\alpha T^2)$$

Typical values (for SiC) α and α_E are $4\text{x}10^{-6}$ and $-32\text{x}10^{-6}$, respectively. Hence, the quadratic terms can be neglected with less than a one percent error for temperature differences up to 2000 K. The resonant frequency change with temperature then becomes

$$1+2\alpha_{fr}T \propto 1+(\alpha_E+\alpha)T \qquad \text{(Eq. 4)}$$

which reduces to

$$2\alpha_{fr} \propto \alpha_E+\alpha \qquad \text{(Eq.5)}$$

The Young's modulus coefficient is negative and larger than the thermal expansion coefficient, which explains the experimentally observed decrease in resonant frequency with temperature. Equation 5 does not include any thermal stress induced in the moving element due to differential thermal expansion between device and substrate, and cannot be used to determine either of the temperature coefficients if the resonating device has large thermal stress.

In the folded beam structure shown in Figure 1 (opposite page), when the suspended element expands with temperature more than the substrate, there is a tensile axial stress induced in the beams anchored to the substrate and a compressive stress in the beams attached to the shuttle.

Analysis Procedure

ANSYS/Multiphysics software predicted the resonant-frequency as a function of temperature for the two devices shown in Figure 2. The type-I device has anchors close together and a small shuttle; the type-II device has a large shuttle with anchors far apart. Type-I devices should have low thermal stress and closely follow Equation 2; type-II devices should have high thermal stress and deviate from Equation 2. The beams are 100 µm long by 2 µm wide in the type-I device and 150 µm by 3 µm in the type-II device.

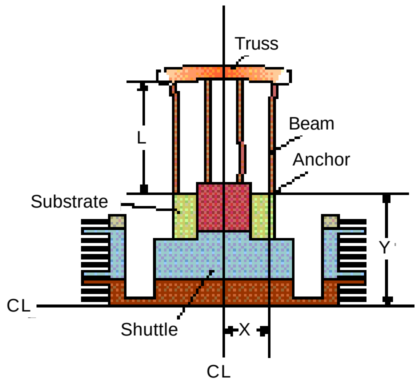

Figure 1: Geometry of folded beam structure

The solid model was built from the ground up in PREP7. Due to the high aspect ratio of MEMS devices, an efficient mesh can be generated using a combination of AMESH and the VSWEEP command (new at Release 5.5), i.e., mesh either the top or bottom device area and then “extrude” this mesh into the solid using VSWEEP. The number of elements through the thickness is determined by EXTOPT, ESIZE. The model includes the substrate region between the anchor locations. This allows the anchor locations to move with the thermal expansion of the substrate. Approximately 12 µm of substrate thickness needs to be modeled. In addition, for accurate results, the product of the substrate thickness and Young’s modulus should be five times greater than the product for the device.

Both models have a 1.5 µm-thick layer of silicon dioxide (SiO_2) on the Si substrate. SiC is then grown on the SiO_2 layer in the type-I device. The type-II device has an extra 3.5-µm layer of polysilicon between the SiO_2 and SiC.

The bottom of the substrate was fixed in the z-direction (normal to the surface) and allowed free x-y thermal expansion in the plane of the device. Two rows of eight-node bricks were used across the thickness of the device. The type-I device was also run with two rows of 20-node bricks. Using 20-node bricks, the lateral mode resonant frequency changes were less than 0.2 percent for all the temperatures compared to the eight-node brick results. Type-II results using one row of eight- or 20-node elements across the thickness were different. These results show that three nodes across the thickness are sufficient for accurate results. One quadratic element containing three nodes should be more accurate than two linear elements with a total of three nodes. Accurate thermal expansion coefficients are necessary for accurate results. Figure 3 shows those values for Si and SiC as a function of temperature. Table 1 gives the other properties used in the analysis. Experimentally determined values for the Young’s modulus temperature coefficient of Si are between -25 and -80ppm/°C and for SiC between -10 and -46 ppm/°C. This study used the largest values.

The analysis was performed in two steps: (1) a static analysis to determine the thermal stress and shape change for an applied, uniform temperature; (2) a modal analysis based on the stress and new shape. Results include temperature-dependent properties, thermal stress, and deformed shape from 300 to 1000 K in steps of 100 K.

Results

The first four mode shapes for the type-I device are shown in Figure 4. For both the type-I and -II devices, the lateral mode is the third, the second mode is out of the plane, and modes one and four are rocking or tilting.

The room-temperature frequencies for each of the devices and mode shapes are given in Table 2.

Figure 5 shows the lateral mode normalized frequency as a function of temperature for the two devices. The normalized Young’s modulus over the 1000 K temperature range drops by 4.5 percent. If the Young’s modulus temperature coefficient was dominant, then the resonant frequency would also decrease by one-half of 4.5 percent (Equation 5). However, the resonant frequency also depends on the coefficient of thermal expansion; since this is positive and nonlinear with temperature, the resonant frequency curve should not decrease as fast as one-half the Young’s modulus curve and should be nonlinear.

The results show that the resonant frequency of the type-I device decreases nonlinearly by 3.5 percent between 300 and 1300 K. Using the

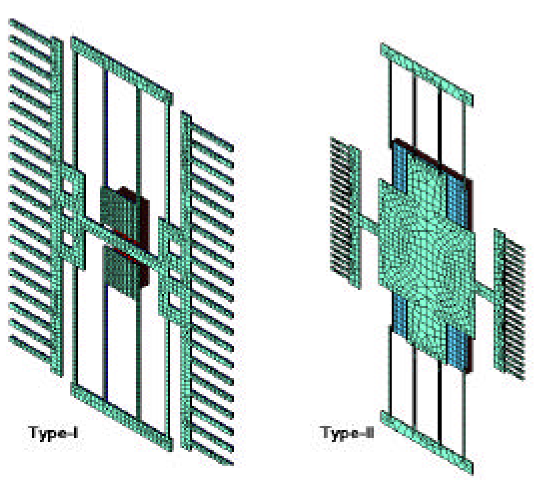

Figure 2: FEM geometry showing type-I and type-II devices

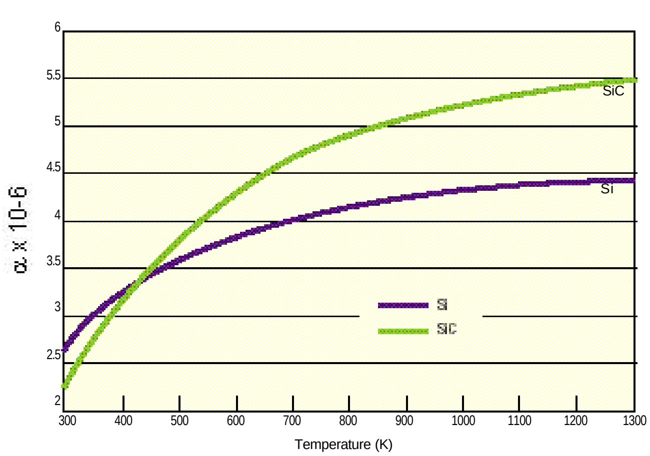

Figure 3: Thermal expansion coefficient of Si and SiC versus temperature

Material	Density Kg/m^3	Young's modulus coefficient 10^{-6}/K	Thermal expansion coefficient 10^{-6}/K	Young's modulus GPa
SiC	3230	-46	Figure 5	250
Si	2320	-80	Figure 5	160
SiO_2	2000	-46	0.734	100

Table 1: Material properties used in the finite element analysis

Device	Resonant Frequency (kHz)			
	Mode 1	Mode 2	Mode 3	Mode 4
Type-I	23	39	43	49
Type-II	7	12	21	25

Table 2: Nominal resonant frequencies for first four modes

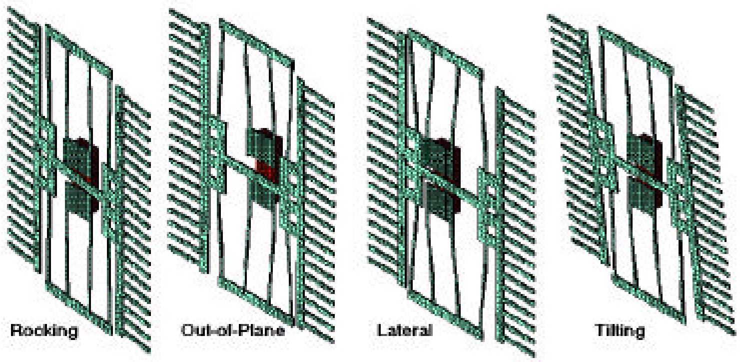

Figure 4: Mode shapes for type-I device

material properties of SiC, this behavior agrees with the theory according to Equation 5. It shows that thermal stress is low in the type-I device and that the substrate material has a negligible effect.

For a type-II device, the resonant frequency versus temperature decreases by 2 percent between 300 and 700 K and then rises slightly with temperature up to 1300 K. This behavior cannot be explained by Equation 5, but may be explained by considering the thermal expansion coefficients of both the SiC device and the Si substrate. Below 700 K, the Si substrate expands faster than the SiC device, generating compressive stress in the outer beams. The inner beams are in tension. Most of the stress occurs in the outer beams because the relatively stiff truss partially isolates the inner beams. The beam stress contributes to the frequency decrease caused by the lower Young's modulus. The frequency drops rapidly. The opposite occurs above 700 K. Above 700 K, the SiC device grows faster than the Si substrate, and the stress in the beams reverses. This offsets the decrease due to the Young's modulus and causes the resonant frequency to remain constant. Preliminary experimental results for these devices show a good correlation with the ANSYS FEA results.

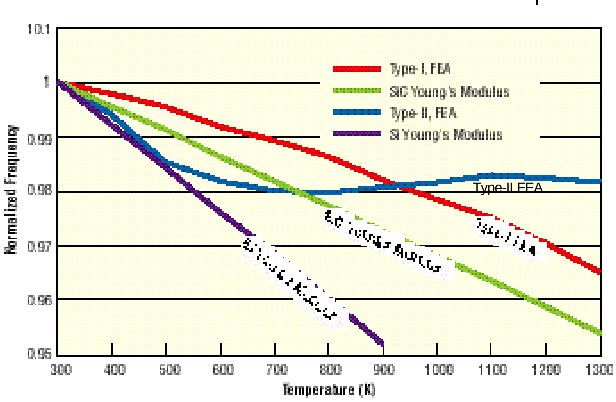

Figure 5: Frequency of the lateral mode versus temperature

Conclusions

In a two-material, lateral-resonating device, anchor spacing and shuttle size influence the resonance frequency with temperature characteristic. A type-I device with closely spaced anchors behaves according to theory (Equation 5) and is not influenced by the thermal expansion of the substrate. This type of device would be suitable for use in a test/validation device to determine the temperature coefficient of Young's modulus. This work shows that for a type-II device (widely spaced anchors), the substrate thermal expansion influences the resonant frequency. High thermal stress develops in the beams, resulting in an unusual frequency versus temperature curve. Note that, for accurate finite element modeling, it is important to include the substrate material between the anchors to allow differential thermal expansion between the device and the substrate. These conclusions only apply to lateral-resonating devices where the material of the suspended or moving element differs from that of the substrate.